Static Loading Analysis of a Double Wishbone Rear Suspension Assembly

Finite Element Analysis Final Project Report

Cade Kaminski

MEGN 324

Colorado School of Mines

Spring 2026

Executive Summary

This report presents a finite element analysis of a rear double wishbone suspension assembly subjected to a representative wheel load applied at the knuckle. The assembly comprises a lower suspension arm and upper suspension arm in AISI 4340 normalized steel with a knuckle, shock clamp, shock plunger, and shock tube in cast carbon steel, and pin connections. Three studies were done. A full assembly with the shock plunger axially fixed inside the tube, a full assembly with the shock plunger free to translate against a spring connector, and a local model of the lower suspension arm only. Hand calculations using free body diagrams established the internal force distribution at every pin location and verified calculations from SWS.

Background

The suspension system of a vehicle isolates the chassis from road inputs while maintaining tire contact and steering geometry under load. A double wishbone configuration uses an upper and lower control arm pinned to the chassis on the inboard side and to the knuckle on the outboard side. Because the control arms and the knuckle constitute unsprung mass, reductions in their weight contribute directly to ride quality and handling response. Any reduction in component mass must, however, preserve the structural margin against static and fatigue failure under the loading conditions seen in service.

This report is a static finite element analysis of a simplified rear suspension assembly. The objective of the study is this. First, the analysis must characterize the stress and displacement field in every load bearing component under a representative wheel load. Second, the analysis must demonstrate that the lower suspension arm, the heaviest of the load bearing parts, retains an adequate factor of safety against yielding so that subsequent design iterations can target weight reduction with confidence.

System Configuration

The simplified rear suspension is a six body assembly. The lower suspension arm pivots at point A on the chassis and connects to the knuckle at point C and to the base of the shock plunger at point B. The upper suspension arm pivots at point G on the chassis and connects to the knuckle at point D. The shock assembly consists of a clamp pinned to the chassis at point E, a shock tube bonded to the clamp, and a plunger that translates inside the tube. A washer piece at the base of the plunger connects to the lower suspension arm at point B. The applied wheel loads are applied to the knuckle at point H, located 0.850 inches outboard of the knuckle to upper arm connection D and 0.500 inches below the upper arm centerline.

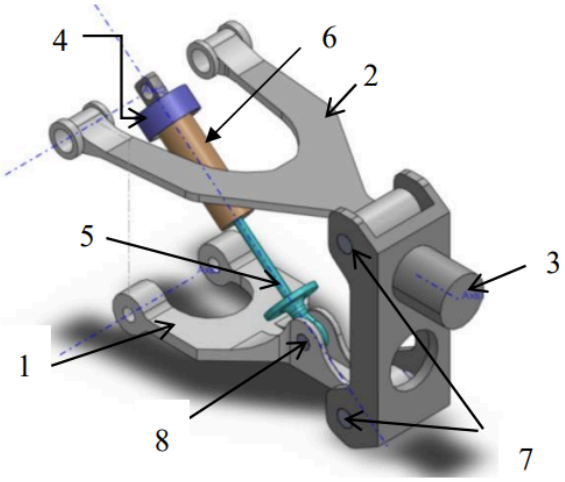

Figure 1: *Isometric rendering of the simplified rear suspension assembly with parts labeled.*

Table 1: *Major geometric dimensions of the suspension assembly.*

Dimension	Value (in)
Vertical distance from A to G	2.700
Horizontal distance from A to B	2.353
Horizontal distance from A to C	3.555
Vertical offset from A to B	0.379
Horizontal distance from G to D	4.136
Horizontal offset from D to H	0.850
Vertical offset from D to H	0.500
Shock clamp axial length	0.350
Shock tube length (clamp to retaining ring)	1.995
Shock plunger axial length	1.969

System Properties

Three materials are assigned to the bodies of the assembly. The lower and upper suspension arms are AISI 4340 steel in the normalized condition. The knuckle, shock clamp, shock plunger, and shock tube are cast carbon steel. The pins between rotating bodies are alloy steel through the SolidWorks pin connector.

System Conditions

Three boundary conditions are applied to the assembly. Hinge fixities at points A, A', G, G', and E represent the pinned connections between the suspension and the vehicle chassis. A pin connector between the shock plunger and the shock tube enforces a constraint, with axial translation either fixed or free. A bonded contact connects the shock clamp to the shock tube since these components are not designed to do anything relative to each other in service. The applied wheel has 35 lbf horizontal force in

the negative x direction applied to the right hand vertical face of the knuckle and a 65 lbf vertical force in the positive y direction applied to the lower half of the horizontal cylindrical face on the knuckle.

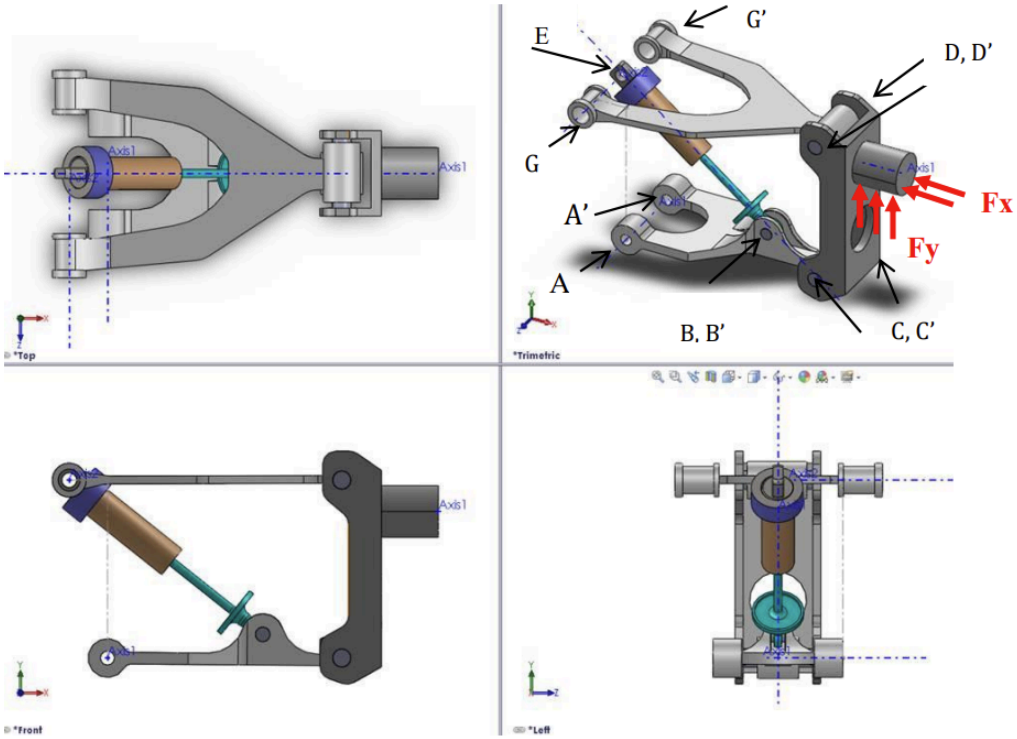

Figure 2: *System conditions for the assembly studies.*

In the second assembly study, an axial spring connector with stiffness k = 800 lbf/in is added between the lower face of the shock clamp and the upper face of the washer at the base of the shock plunger.

In the local lower arm study, all parts other than the lower suspension arm are excluded from the analysis. The hinge fixity at A and A' is preserved. Loads at B and C are applied directly to half cylindrical surfaces created by split lines too. The applied loads are taken from the equilibrium calculations. A soft spring stabilization option was enabled in the study properties to remove the rigid body rotation mode about the hinge axis.

System Discretization

The default global element size for a standard mesh produced was used as the starting point for the assembly studies. A mesh control was applied to the cylindrical contact surfaces between the shock plunger and the shock tube as well.

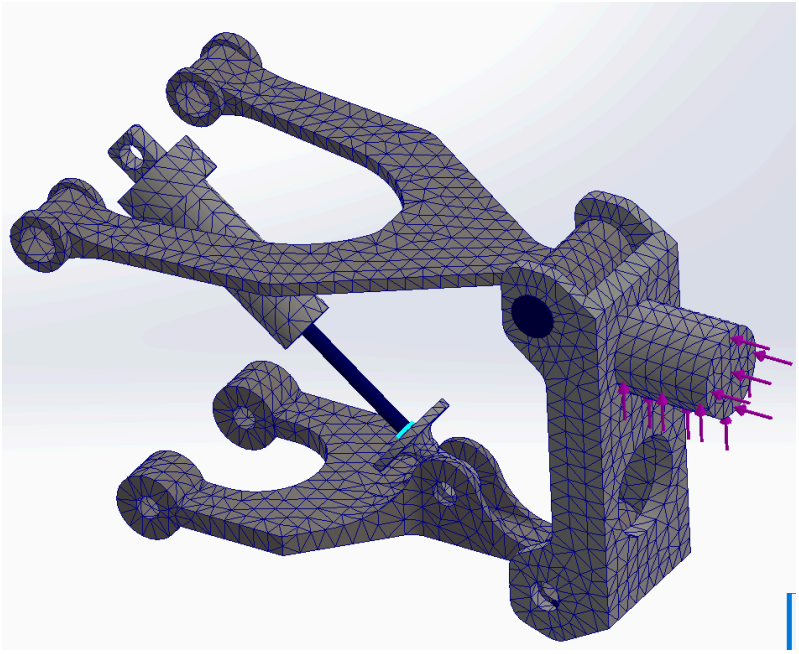

Figure 3a: *Final mesh applied to the spring supported assembly study.*

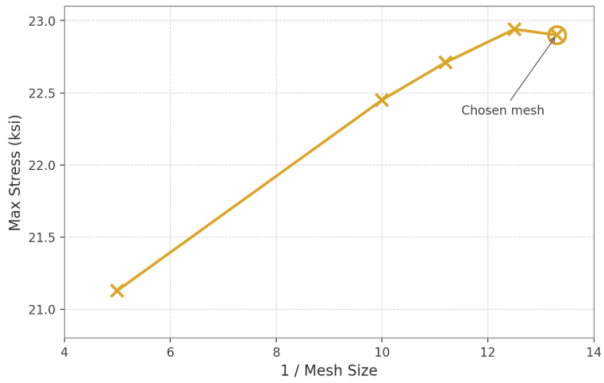

Figure 3b: *Mesh convergence study for the peak von Mises stress on the lower arm.*

The mesh convergence study was performed by running the local lower arm study at four global element sizes.

Validation and Verification

Suspension Assembly

Free body diagrams of the upper arm, knuckle, lower arm, and shock assembly were used to find the internal pin reactions in terms of the applied loads. The upper arm has only two pin connections, at G and D, and is therefore a two force member that carries axial load along the line GD. Because G and D lie at the same y coordinate, the line GD is horizontal and the upper arm force is only in the x direction. The shock and plunger assembly likewise has two pin connections, at E on the chassis and at B on the lower arm, and is a two force member acting along the line EB. The knuckle has two pin connections, at D and

C, with the applied loads at H, and provides three equations of equilibrium. The lower arm has three pin connections, at A, B, and C, and provides another three equations of equilibrium.

Table 4: *Magnitudes of internal pin reactions from equilibrium analysis.*

Pin	x component (lbf)	y component (lbf)	Resultant (lbf)
A	117.1	16.6	118.3
B	103.1	81.6	131.5
C	14.0	65.0	66.5
D	49.0	0.0	49.0
E	103.1	81.6	131.5
G	49.0	0.0	49.0

Spring Element Model of the Shock

A one dimensional spring element model of the shock absorber was constructed to predict the deformation of the shock under the calculated 131.5 lbf compressive load. The shock is modeled as a chain of axial spring elements representing the clamp, the tube, and the plunger, with an optional spring connector representing the helical coil spring in the second study configuration. The clamp, tube, and plunger spring constants are calculated from the formula k = AE/L. All the MOM hand calcs are in Appendix A.

Experimental Validation Plan

Experimental validation of the computational model would proceed by mounting the physical assembly to a rigid test fixture that reproduces the chassis pin connections at A, G, and E. A static load cell or hydraulic actuator would apply a controlled vertical load of 65 lbf to the knuckle force application point H, and a separate horizontal load cell would apply a controlled 35 lbf horizontal load. Strain gauges placed on the lower suspension arm in the regions of predicted maximum stress (along the curved edges between B and C identified in the project description) would measure the local strain field. Linear variable differential transformer (LVDT) sensors would measure the displacement of the knuckle in the y direction and the compression of the shock between the clamp and the plunger washer. The measured strain values multiplied by the elastic modulus would be compared directly to the FEA peak σ_x stress, the LVDT shock compression would be compared to the spring 1D model deformation of -0.164 inches, and the LVDT knuckle displacement would be compared to the peak y displacement reported by the FEA. Repeating the test under at least three different load levels (for example, half, full, and 1.5 times the design load) would allow the linearity of the response to be checked and the FEA to be validated across the design envelope.

Results

Three SolidWorks Simulation studies were executed and the peak stresses, peak displacements, and minimum factors of safety are reported below. Stresses are evaluated using the von Mises yield criterion, which combines the deviatoric components of the stress tensor into a single scalar suitable for comparison with the uniaxial yield strength of a ductile material.

Assembly with Fixed Shock

Study name	Stiff* (-Default-)
DetailsMesh type	Solid Mesh
Mesher Used	Standard mesh
Automatic Transition	Off
Include Mesh Auto Loops	Off
Jacobian points for High quality mesh	16 points
Mesh Control	Defined
Element size	0.155418 in
Tolerance	0.00777092 in
Mesh quality	High
Total nodes	22555
Total elements	11529
Maximum Aspect Ratio	39.926
Percentage of elements with Aspect Ratio < 3	87.2
Percentage of elements with Aspect Ratio > 10	0.104
Percentage of distorted elements	0
Number of distorted elements	0
Remesh failed parts independently	Off
Time to complete mesh(hh:mm:ss)	00:00:03

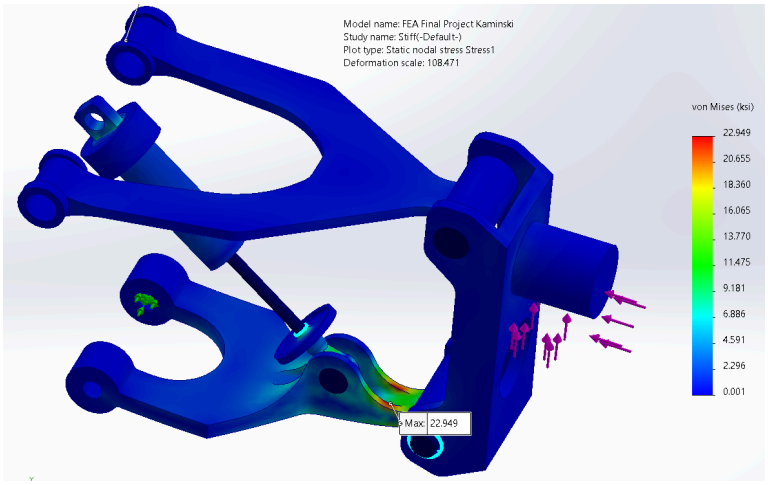

Figure 7: *Von Mises stress on the lower suspension arm in the fixed shock study and details.*

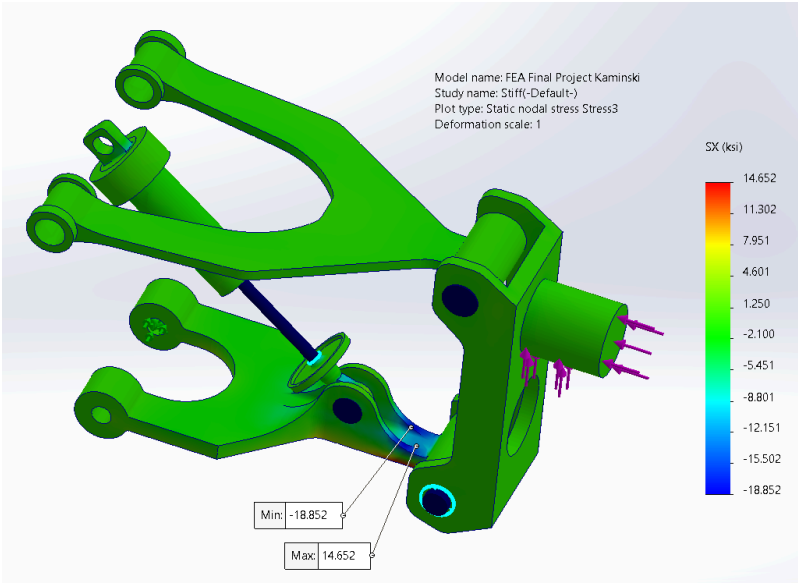

Figure 8: *Normal stress σ_x on the lower suspension*

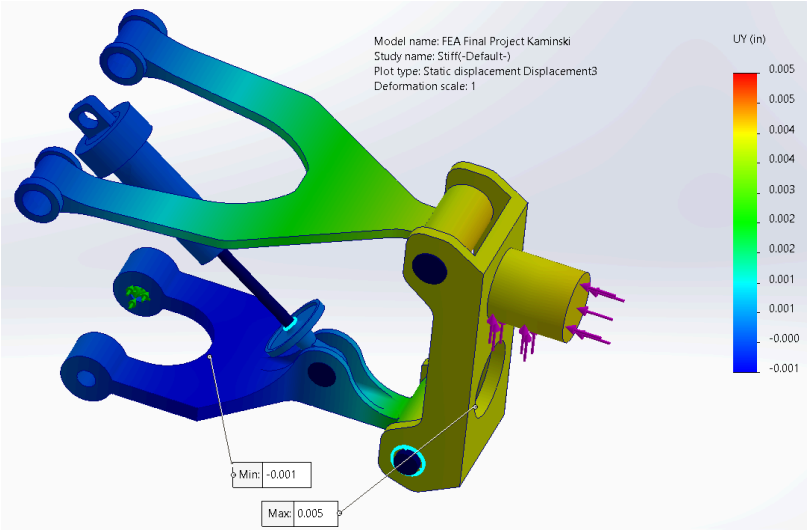

Figure 9: *Vertical (y) displacement field on the assembly in the fixed shock study.*

Table 6: *Peak results from the fixed shock assembly study.*

Quantity	Value
Peak σ_vM, lower arm (ksi)	22.9
Peak σ_x, lower arm (ksi)	-18.9
Absolute max y displacement (in)	5.46

Assembly with Spring Shock

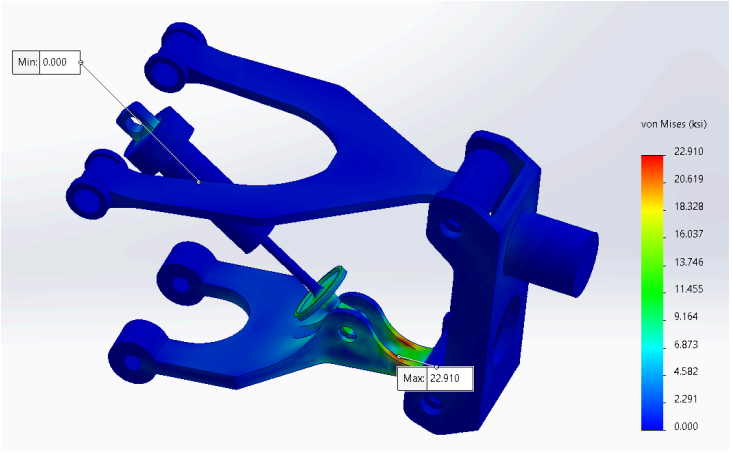

Study name	Spring* (-Default-)
DetailsMesh type	Solid Mesh
Mesher Used	Standard mesh
Automatic Transition	Off
Include Mesh Auto Loops	Off
Jacobian points for High quality mesh	16 points
Mesh Control	Defined
Element size	0.155418 in
Tolerance	0.00777092 in
Mesh quality	High
Total nodes	22593
Total elements	11536
Maximum Aspect Ratio	39.927
Percentage of elements with Aspect Ratio < 3	87.1
Percentage of elements with Aspect Ratio > 10	0.0954
Percentage of distorted elements	0
Number of distorted elements	0
Remesh failed parts independently	Off
Time to complete mesh(hh:mm:ss)	00:00:03

Figure 10: *Von Mises stress on the lower suspension arm in the spring shock study and details.*

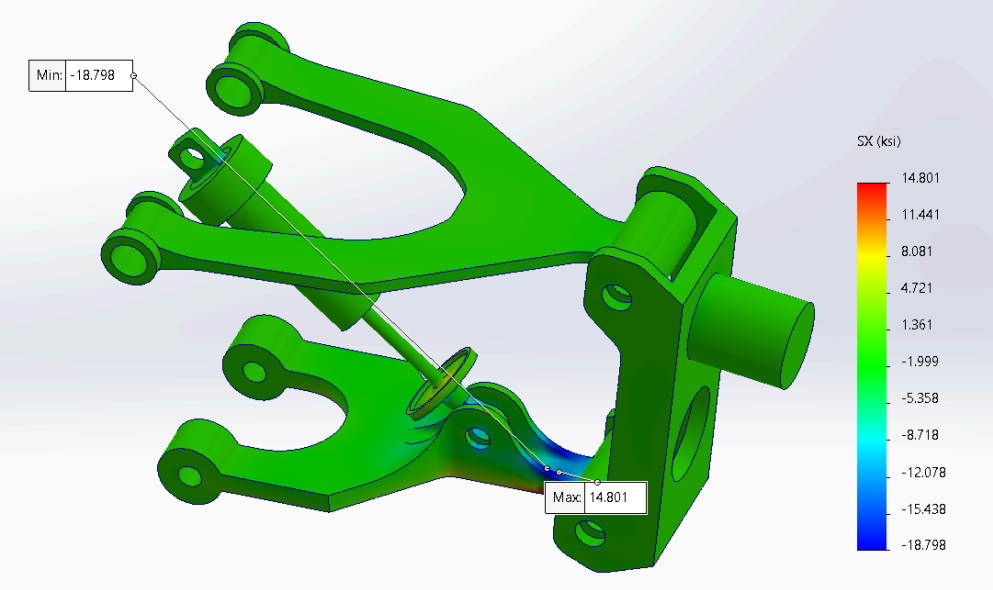

Figure 11: *Normal stress σ_x on the lower suspension arm in the spring shock study, with probe locations along the curved edges between B and C.*

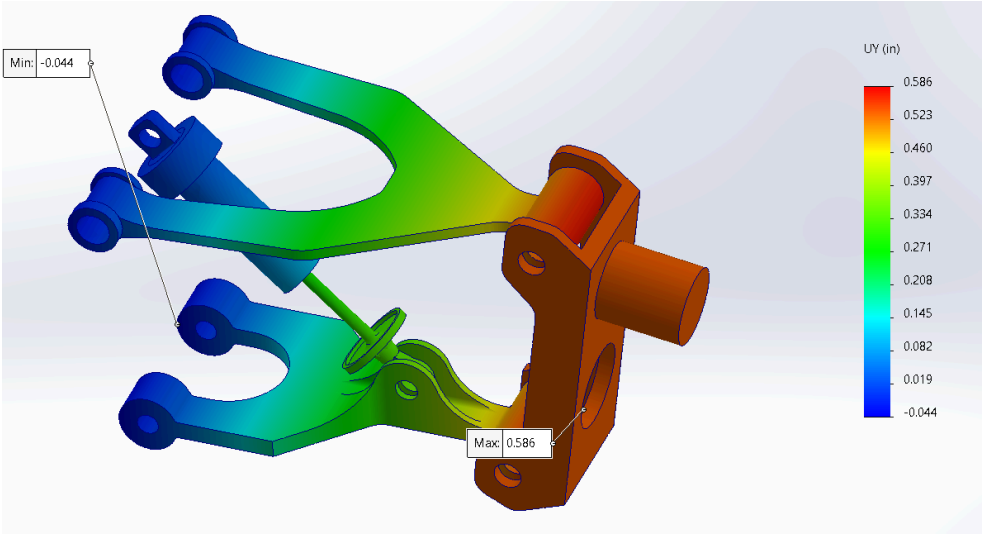

Figure 12: *Vertical (y) displacement field on the assembly in the spring shock study.*

Table 7: *Peak results from the spring shock assembly study.*

Quantity	Value
Peak σ_vM, lower arm (ksi)	22.9
Peak σ_x, lower arm (ksi)	-18.9
Absolute max y displacement (in)	0.586

Local Lower Arm Study

In the local lower arm study, the upper arm, knuckle, and shock components were excluded from the simulation and the equilibrium reactions calculated above were applied directly to half cylindrical surfaces at B and C. The split lines were oriented perpendicular to the line of action of the resultant pin force at each location. At B, the resultant force has magnitude 131.5 lbf and the split line is therefore oriented 38.4 degrees from horizontal so that the loaded half of the cylindrical surface lies on the side that the resultant pushes into. There are also two split lines at point

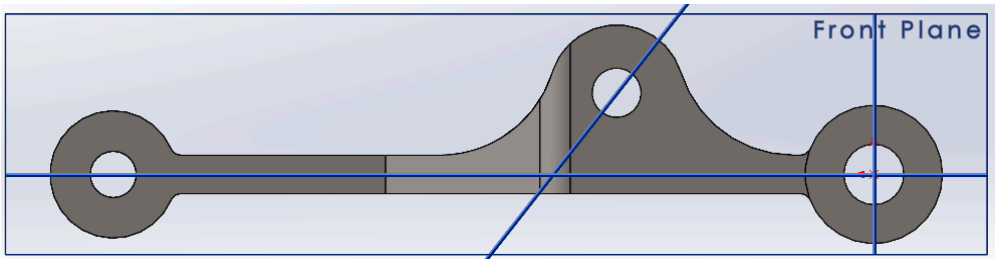

Figure 13: *Split lines at B and C on the lower suspension arm.*

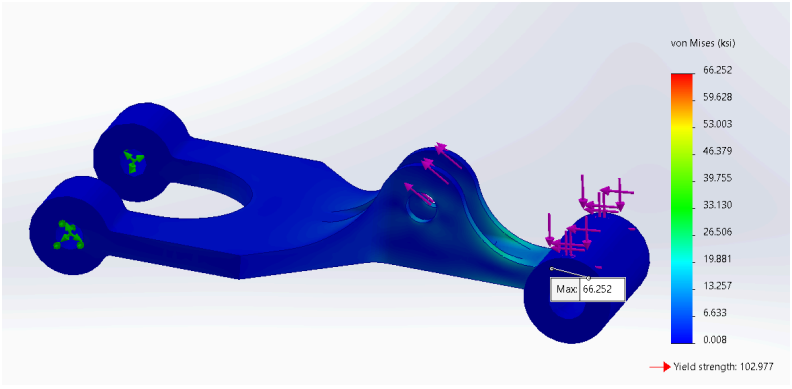

Study name	Static 1* (-Default-)
DetailsMesh type	Solid Mesh
Mesher Used	Standard mesh
Automatic Transition	Off
Include Mesh Auto Loops	Off
Jacobian points for High quality mesh	16 points
Element size	0.100053 in
Tolerance	0.00500263 in
Mesh quality	High
Total nodes	134244
Total elements	89762
Maximum Aspect Ratio	11.695
Percentage of elements with Aspect Ratio < 3	98.9
Percentage of elements with Aspect Ratio > 10	0.025
Percentage of distorted elements	0
Number of distorted elements	0
Time to complete mesh(hh:mm:ss)	00:00:01

Figure 14: *Von Mises stress on the lower suspension arm in the local study.*

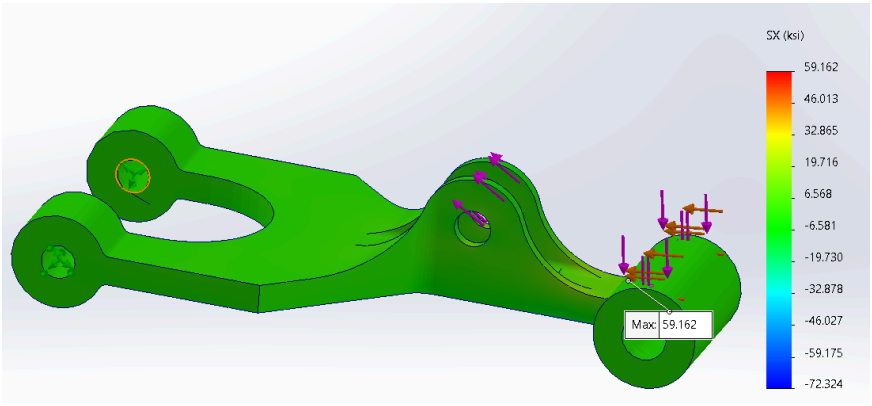

Figure 15: *Normal stress σ_x on the lower suspension arm in the local study with probe along the curved edges.*

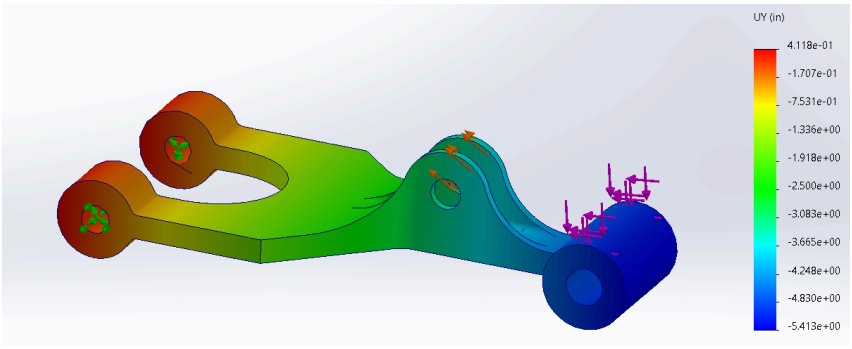

Figure 16: *Vertical (y) displacement on the lower arm in the local study.*

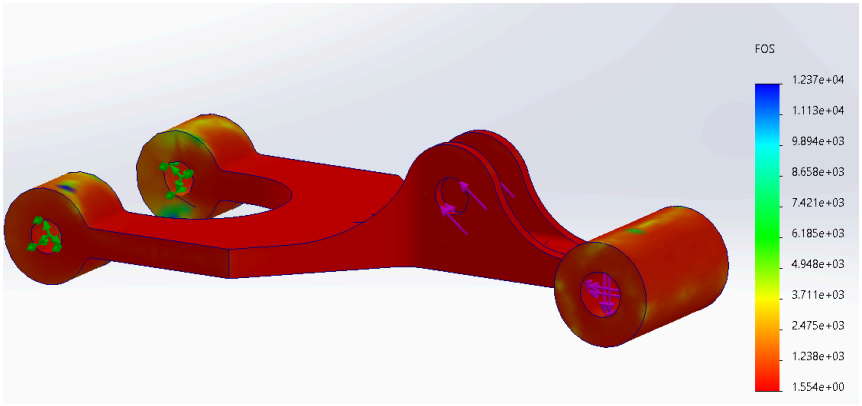

Figure 17: *Factor of safety distribution on the lower arm using the von Mises yield criterion.*

Table 8: *Peak results from the local lower arm study.*

Quantity	Value
Peak σ_vM (ksi)	66.52
Maximum σ_x (ksi)	59.1
Absolute max y displacement (in)	0.421
Minimum factor of safety	1.55

MoM Verification of Peak σ_x

To verify the FEA peak σ_x on the lower arm, an analytic mechanics of materials estimate was constructed at the location of the FEA maximum. A section cut perpendicular to the local axis of the arm was taken at that location, and the cross sectional area A and second moment of area I_zz about the centroidal axis were measured in Section Properties. The internal forces at the section were obtained from a free body diagram that isolates one side of the cut, with the applied forces at B and C from the equilibrium analysis applied to the appropriate side.

Discussion

Comparison of Assembly Simulations

The two assembly studies differ only in how the shock subassembly is treated. In the fixed configuration the plunger is bonded to the tube and the shock acts as a rigid link between E and B. In the spring configuration the plunger slides freely in the tube and the 800 lbf/in spring connector is the only element resisting axial compression of the shock. Because the equilibrium that determines the pin reactions is identical between the two studies, the peak von Mises stress on the lower arm should also be identical, and the FEA confirms this. Both studies report a peak of 22.9 ksi on the lower arm and a peak σ_x of -18.9 ksi at the same location. The displacement field, by contrast, differs dramatically. The fixed shock study produces an absolute peak y displacement of 5.46 thousandths at the knuckle, while the spring shock study produces 0.586 in at the knuckle. The 0.580 in difference is the displacement at the knuckle that results from the shock compressing under load. The 1D spring model predicted 0.164 in of axial compression at the shock; the additional displacement at the knuckle is the rigid body rotation of the lower arm about pin A that the shock compression permits, amplified by the lever arm from A out to the knuckle force application point at H.

Local Lower Arm Model versus Assembly Spring Model

The local lower arm study returned a peak von Mises stress of 66.5 ksi, nearly three times the 22.9 ksi reported by the assembly study. Three sources contribute to this gap. First, the local model uses a far finer mesh (134k nodes versus 22k nodes for the assembly), which resolves stress concentrations along the fillets and the split line edges that the assembly mesh smears across larger elements. Second, the local model applies the equilibrium resultant as a uniform distribution across half cylindrical split surfaces, which concentrates load over a smaller area than the contact based load distribution that the assembly study's pin connectors generate. Third, the split surface load application introduces a small artificial stress concentration at the split line edges themselves where the pressure jumps discontinuously from loaded to unloaded. The local model is therefore expected to be more conservative than the assembly study, but the magnitude of the difference observed here is large enough to warrant verification. A useful check, recommended for follow up work, would be to refine the assembly mesh in the lower arm region until its peak stress reading begins to climb toward the local model value, and to confirm that the locations of the peaks coincide between the two studies. The minimum factor of safety reported by the local study is 1.55, which falls below the project requirement of 3.5 by a substantial margin and shows that the current lower arm geometry is not good for the specified load case. Whether this holds depends on which model better represents the physical part. If the local result is artificially inflated by the load application method, the assembly result of σ_vM = 22.9 ksi against a 145 ksi yield strength gives a factor of safety of approximately 6.3, which exceeds the requirement comfortably.

Conclusions

This report has presented a complete static finite element analysis of a simplified rear double wishbone suspension assembly subjected to a planar wheel load of 35 lbf horizontal and 65 lbf vertical at the knuckle. The equilibrium analysis established that the upper arm acts as a two force member carrying 49 lbf in compression along the line GD, that the shock acts as a two force member carrying 131.5 lbf in compression along the line BE, and that the resulting pin reactions at A, B, and C on the lower arm are 118.3, 131.5, and 66.5 lbf in magnitude respectively. A one dimensional spring element analysis predicted shock deformations of 0.583 thousandths of an inch with the plunger fixed to the tube and 164.4 thousandths of an inch with the plunger sliding against the 800 lbf/in helical spring.

The three FEA studies confirmed the equilibrium predictions and identified the lower suspension arm as the principal load bearing component. The fixed and spring assembly studies both produced a peak von Mises stress of 22.9 ksi on the lower arm with a peak σ_x of -18.9 ksi at the same location. The local lower arm study produced a peak von Mises stress of 66.5 ksi and a minimum factor of safety of 1.55 against yielding of the AISI 4340 normalized steel using the von Mises yield criterion. The discrepancy between the local and assembly results is large enough that the design margin against yielding cannot be stated with full confidence from this work alone; the assembly result implies a factor of safety of approximately 6.3 while the local result of 1.55 falls below the project requirement of 3.5. Resolving this gap with a refined assembly mesh and a load application sensitivity study is the most important immediate next step before any weight reduction effort proceeds.

Future work should extend the analysis to include dynamic load cases representative of bump, cornering, and braking events; evaluate the fatigue life of the lower arm under realistic load spectra; and perform a coupled assembly optimization that considers the mass and stiffness of all six bodies simultaneously rather than treating the lower arm in isolation.

References

[1] SolidWorks Simulation Material Library, Dassault Systèmes SOLIDWORKS Corporation, version 2024.

[2] R. C. Hibbeler, *Statics and Mechanics of Materials*, 5th ed., Pearson, 2017.

[3] MEGN 324 Final Project Description, Colorado School of Mines, Spring 2026.

Appendix B: Hand Calculations

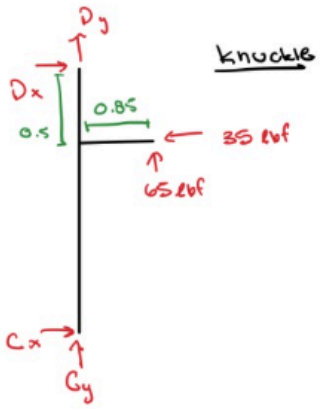

$M_c = 35(2.2) + 65(0.85) + D_x(2.7)$

$D_x = -48.98$ lbf

$D_y = 0$

$\Sigma F_x = -35 + 48.98 + C_x = 0$

$C_x = -13.98$ lbf

$\Sigma F_y = C_y + 65 = 0$

$C_y = -65$ lbf

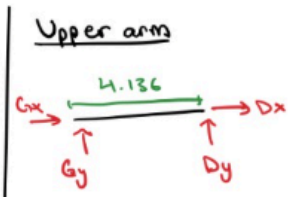

$\Sigma F_y = G_y + D_y = 0$

$G_y = 0$

$\Sigma F_x = G_x + D_x = 0$

$G_x = 48.98$

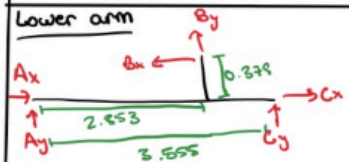

$\Sigma M_A = F_B \cos(38.3)(0.379) + F_B \sin(38.3)(2.853) + C_y(3.585) = 0$

$B_x = 103.2$ lbf

$B_y = 81.6$ lbf

$\Sigma F_x = A_x + B_x + C_x = 0$

$A_x = 117.2$ lbf

$\Sigma F_x = A_y + B_y + C_y = 0$

$A_y = -16.6$ lbf

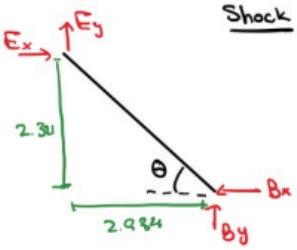

$\Sigma F_x = E_x - B_x = 0$

$E_x = 105.2$ lbf

$\Sigma F_y = E_y + B_y = 0$

$E_y = -81.6$ lbf

$P = F_B$ (Fixed)

$$\delta = \frac{PL}{AE} + \frac{PL}{AE} = \frac{131.609(1.215)}{0.01224(29007.5)} + \frac{(131.61)(4.496)}{(0.0702)(29007.5)}$$

$$= -0.000\,83483$$

Spring

$F = kx$

$x = \frac{F}{k} = \frac{131.61}{800} = -0.1645$